Nanoscale

Accepted Manuscript

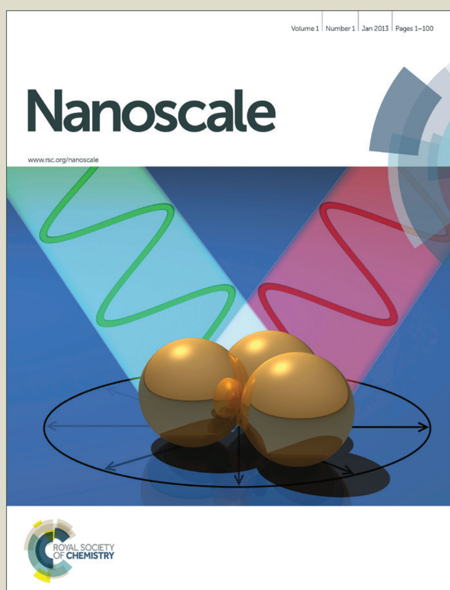

This is an *Accepted Manuscript*, which has been through the Royal Society of Chemistry peer review process and has been accepted for publication.

Accepted Manuscripts are published online shortly after acceptance, before technical editing, formatting and proof reading. Using this free service, authors can make their results available to the community, in citable form, before we publish the edited article. We will replace this *Accepted Manuscript* with the edited and formatted *Advance Article* as soon as it is available.

You can find more information about *Accepted Manuscripts* in the Information for Authors.

Please note that technical editing may introduce minor changes to the text and/or graphics, which may alter content. The journal's standard Terms & Conditions and the Ethical guidelines still apply. In no event shall the Royal Society of Chemistry be held responsible for any errors or omissions in this *Accepted Manuscript* or any consequences arising from the use of any information it contains.

ROYAL SOCIETY OF CHEMISTRY

www.rsc.org/nanoscale

Nanoscale RSCPublishing

ARTICLE

Novel chemical route for atomic layer deposition of MoS_2 thin film on SiO_2/Si substrate

Cite this: DOI: 10.1039/x0xx00000x

Received 00th January 2012,
Accepted 00th January 2012

DOI: 10.1039/x0xx00000x

www.rsc.org/

Zhenyu Jin,[a,†] Seokhee Shin,[a,†] Do Hyun Kwon,[a] Seung-Joo Han[a] and Yo-Sep Min[a,*]

Recently MoS_2 with a two-dimensional layered structure has attracted great attention as an emerging material for electronics and catalysis applications. Although atomic layer deposition (ALD) is well-known as a special modification of chemical vapor deposition in order to grow a thin film in a manner of *layer-by-layer*, there is little literature on ALD of MoS_2 due to a lack of suitable chemistry. Here we report MoS_2 growth by ALD using molybdenum hexacarbonyl and dimethyldisulfide as Mo and S precursors, respectively. MoS_2 can be directly grown on SiO_2/Si substrate at 100 ^{o}C via the novel chemical route. Although the as-grown films are amorphous in X-ray diffraction analysis, they clearly show characteristic Raman modes (E^1_{2g} and A_{1g}) of 2H-MoS_2 with a trigonal prismatic arrangement of S-Mo-S units. After annealing at 900 ^{o}C for 5 min under Ar atmosphere, the film is crystallized for MoS_2 layers to be aligned with its basal plane parallel to the substrate.

Nanoscale Accepted Manuscript

1 Introduction

Due to the success in recent research on graphene and its various applications,[1] two-dimensional (2D) materials such as transition metal dichalcogenides (TMDs) have attracted great attention in academia and industry.[2-3] Among the TMDs (MX_2) where M is a transition metal of groups 4-10 and X is a chalcogen, MoS_2 is one of potential materials for electronics and catalysis applications.[4-5] While bulk MoS_2 is an n-type semiconductor with an indirect bandgap (~1.3 eV), the atomic monolayer of MoS_2 have a direct bandgap (~1.8 eV).[6] Several groups reported performance of MoS_2 in field effect transistors and logic devices in which a monolayer or a film of MoS_2 were used as a semiconducting channel in the transistor, instead of silicon.[7-9] In addition, MoS_2 is a strong candidate to replace expensive Pt catalyst in electrochemical hydrogen evolution reaction (HER) for renewable H_2 production.[10-11]

For the electronic device applications of 2D materials, they should have a bandgap to ensure a high on/off ratio of transistor, and should be directly grown with a high crystallinity on an insulating material (e.g., SiO_2). However, since graphene has intrinsically no bandgap and cannot be grown without a catalytic film (e.g., Ni and Cu), the performance of the graphene transistor is not as excellent as expected from theoretical calculations and the best experimental mobility (10^5 cm^2/Vs) obtained by using an exfoliated graphene.[12] It was recently reported that monolayer or ultrathin film of MoS_2 could be directly grown on an insulator without any catalyst by chemical vapor deposition (CVD).[13-16] However, a common problem of their CVD methods is that elemental sulfur is used as a sulfur precursor for MoS_2 CVD. Vapor pressure of the elemental sulfur is ~10^{-5} torr at 40 ^{o}C, which is much lower in comparison to typical vapor pressures of CVD precursors.[17] Even though large-area MoS_2 monolayers were demonstrated by the CVD method, it cannot be utilized in mass production due to a lack of reliability and reproducibility of the process.

On the other hand, atomic layer deposition (ALD) is a special modification of CVD to grow a thin film via self-limiting mechanism.[18] In CVD, while two precursors (e.g., Mo and S precursors) are simultaneously supplied to a substrate, they are alternately exposed onto the substrate and subsequently purged for each precursor in ALD. Therefore one ALD cycle generally consists of two half reactions, which are achieved by repeating four steps (the first precursor exposure and purging steps for the first half reaction and the second precursor exposure and purging steps for the second half reaction). In addition, growth temperature in ALD is maintained to be low enough in order to avoid thermal decomposition of the precursors. Consequently, the film grows with the number of ALD cycles via chemisorption of each precursor which occurs

This journal is © The Royal Society of Chemistry 2013

in turn repeatedly. Considering the principle of ALD based on chemisorption, it is expected that ALD may be an excellent tool for the layered MoS_2.

Recently, MoO_3 thin film was grown by ALD using molybdenum hexacarbonyl ($Mo(CO)_6$) and various oxidants.[19] ALD of Mo thin film was also reported by using MoF_6 and Si_2H_6.[20] MoS_2 HER catalyst was prepared by sulfurizing MoO_3 thin film which was grown by ALD from $Mo(CO)_6$ and ozone.[21] Very recently, the first report on ALD of MoS_2 was presented by Loh, et al. by using $MoCl_5$ and H_2S on sapphire substrates.[22] To the best of our knowledge, this is the only paper for MoS_2 ALD ever reported, due to a lack of suitable chemistry for ALD. Here we present a novel chemical route for MoS_2 ALD in which MoS_2 can be directly grown on a SiO_2/Si substrate using $Mo(CO)_6$ and dimethyldisulfide (CH_3SSCH_3, DMDS) as Mo and S precursors, respectively.

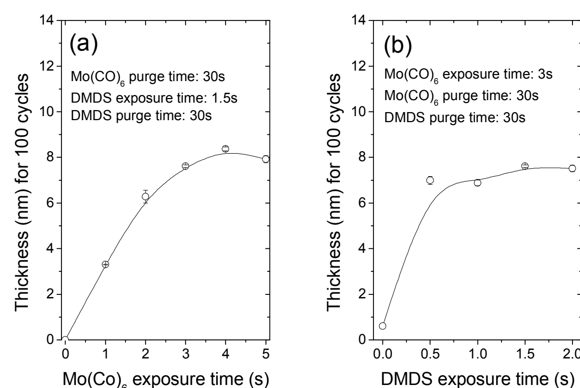

Fig. 1. Thicknesses of MoS_2 films against exposure times of $Mo(CO)_6$ (a) and DMDS (b). ALD was performed at 100 °C for 100 cycles. The curves are drawn for eye-guide.

2 Experimental

In order to investigate the growth behavior of MoS_2 using the novel chemistry of ALD, thin films were simultaneously grown on both SiO_2 (300 nm)/Si (1×1 or 2×2 cm^2) and bare Si wafers in a laminar flow type ALD reactor. The films grown on the bare Si were used to measure the thickness by spectroscopic ellipsometry (SE). $Mo(CO)_6$ and DMDS (Aldrich) were vaporized from external canisters at room temperature and led into the reactor through solenoid valves with a carrier gas of N_2 (100 sccm, 99.999%) for $Mo(CO)_6$ and without any carrier gas for DMDS. The doses of $Mo(CO)_6$ and DMDS were ~1.8×10^{-6} and ~4.0×10^{-4} mol/s, respectively. For purging the reactor, N_2 gas was used with a flow rate of 300 sccm. All delivery lines were maintained at 80 °C. The growth temperature was controlled by using a lamp heater, and monitored with a thermocouple which is closely placed to the specimen. The base pressure of the reactor was less than 10 mTorr and ALD was processed at a working pressure range of 1.4 ~ 3.3 Torr.

All thicknesses of the grown films were measured by SE (MG-1000, NanoView). The incident angle of the polarized light in the SE was fixed at around 70°, and the incident light has a spectral range of 1.5 ~ 5.0 eV. The measured data by SE was fitted with a Tauc-Lorentz dispersion function in order to determine the thickness.[23] Raman spectroscopy (Alpha 500R, WiTec) was used to characterize MoS_2 films using a 532 nm laser excitation. The Si peak at 521 cm^{-1} was used as a reference for wavenumber calibration. X-ray photoelectron spectroscopic (XPS) spectra were obtained on a PHI 5000 Versaprobe (ULVAC PHI) using monochromatic Al Kα emission. Binding energies were measured using the C 1*s* peak (284.8 eV) of the adventitious carbon as an internal standard. X-ray diffraction (XRD) measurements were carried out in θ/2θ scan mode using a Philips X'pert Pro MRD X-ray diffractometer with Cu Kα emission. High resolution transmission electron microscopy (HR-TEM) sample was prepared by using a focused ion beam and its microstructure was imaged in a TITAN TM 80-300 FEI microscope.

3 Results and discussion

3.1 Self-limiting growth of MoS_2 thin film by ALD

Although $Mo(CO)_6$ is a solid at ambient condition, it has a vapor pressure of 0.10 ~ 0.15 Torr at room temperature which is enough for deposition process in vacuum.[24,25] Several groups have used $Mo(CO)_6$ as a Mo precursor in ALD or CVD of MoO_3 thin films.[19,26,27] It is well known that physisorbed $Mo(CO)_6$ undergoes decarbonylation to form chemisorbed subcarbonyls, $Mo(CO)_n$ ($n \leq 5$), on the surface of various substrates.[28-31] Therefore $Mo(CO)_6$ was chosen as a Mo precursor for the first-half reaction of ALD.

Chemisorption of organosulfur compounds (e.g., DMDS) has been intensively studied due to their importance in hydrodesulfurization catalysis, self-assembled monolayers and so on.[32,33] There are several reports for dissociative chemisorption of DMDS through S-S bond cleavage to form methylthiolate intermediate (CH_3S-) on the surface of various substrates.[32-36] The surface methylthiolates can undergo additional decomposition via C-S bond cleavage to produce sulfur adatoms releasing gaseous molecules such as $(CH_3)_2S$ and CH_3CH_3. This reaction is utilized in thiol desulfurization by using Mo, Sulfided Mo, or $Mo(CO)_6$ catalysts.[33] Because it is expected that the formation of surface S atoms from the methylthiolates may be also catalyzed by the chemisorbed $Mo(CO)_n$, DMDS was selected as a S precursor for the second-half reaction of ALD. As a result, the chemistry for our MoS_2 ALD may consist of the first- and second-half reactions given in Eqs. 1 and 2:

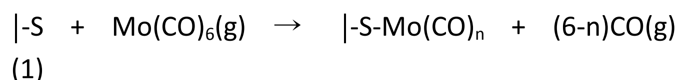

$$|\text{-S} + Mo(CO)_6(g) \rightarrow |\text{-S-}Mo(CO)_n + (6-n)CO(g) \quad (1)$$

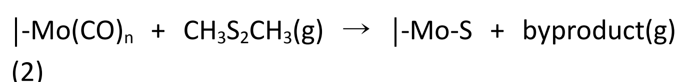

$$|\text{-}Mo(CO)_n + CH_3S_2CH_3(g) \rightarrow |\text{-Mo-S} + \text{byproduct}(g) \quad (2)$$

Nanoscale Accepted Manuscript

This journal is © The Royal Society of Chemistry 2012

where |- denotes surface.

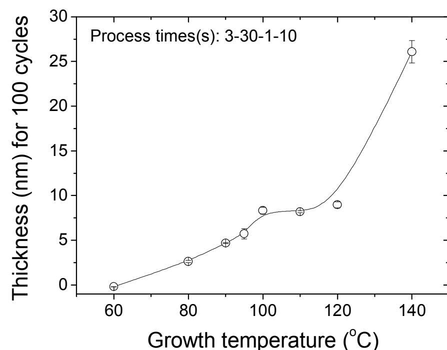

Fig. 2. Thickness of MoS_2 films against growth temperature. ALD was performed for 100 cycles with the process times given in the figure. The curves are drawn for eye-guide.

In order to confirm the self-limiting chemisorption of the precursors in each half-reaction, thicknesses of the films grown at 100 °C for 100 cycles were plotted against exposure times of $Mo(CO)_6$ and DMDS in Fig 1. The chemisorption of $Mo(CO)_6$ in the first-half reaction (Fig. 1a) shows the typical self-limiting growth at longer exposure times (x) of $Mo(CO)_6$ than 3 s due to the saturation of adsorption sites occupied by $Mo(CO)_n$. Similarly, DMDS also follows the self-limiting growth mechanism as shown in Fig. 1b, however the thickness saturates in a much shorter exposure time (y) owing to its high vapor pressure (~29 Torr at room temperature).[37] In addition, when one of both half-reactions was performed with only one precursor by making the exposure time of the other precursor be zero, the thickness increase by a deposit was negligible as shown with the thicknesses at x = 0 (Fig. 1a) or y = 0 (Fig. 1b). Consequently, we can exclude the possibility of uncontrolled thermal decomposition of both precursors in the film growth. It should be noted that when only DMDS was exposed without the exposure of $Mo(CO)_6$ (i.e., x = 0), the thickness of the deposit was also zero. However when the DMDS was exposed on the surface $Mo(CO)_n$ (i.e., x > 0), the film can grow as shown in Fig. 1a. This is an evidence which reveals that the decomposition of the methylthiolate via C-S bond cleavage is also catalyzed by $Mo(CO)_n$, as done by $Mo(CO)_6$.[33]

Generally, film growth by ALD shows a particular temperature window in which the growth-per-cycle (GPC) is weakly dependent on the growth temperature.[18] Figure 2 shows the film thicknesses grown for 100 cycles (x = 3 s and y = 1 s) at different temperatures. Film growth is negligible at 60 °C. However, as the growth temperature becomes higher, the film thickness increases with the growth temperature and then saturates at 100 °C. The typical plateau of the GPC is observed in a temperature range of 100 ~ 120 °C. ALD process at higher temperatures than 120 °C results in a rapid increase of the GPC due to the uncontrolled thermal decomposition of precursors.

In addition, due to the self-limiting nature of ALD, the film thickness linearly increases with the number of ALD cycles. This is a great advantage of ALD because the thickness of the film can be controlled in an angstrom scale by the number of ALD cycles with a value of GPC. Fig. 3a shows thicknesses of MoS_2 films against the number of ALD cycles. The GPC of MoS_2 at 100 °C was evaluated to be 0.11 ± 0.01 nm/cycle (when x = 4 s and y = 1.5 s) from the slope in the figure.

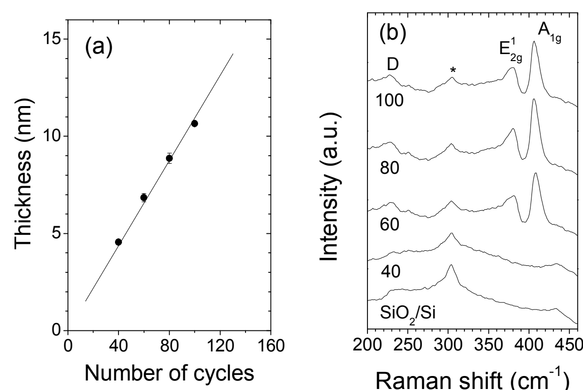

Fig. 3. (a) Thickness of MoS_2 films against number of ALD cycles. (b) Raman spectra (532 nm laser excitation) of MoS_2 films which were grown for various numbers of ALD cycles (the numbers on each spectrum). ALD was performed on SiO_2/Si at 100 °C (x = 4 s and y = 1.5 s).

3.2 Characterization of MoS_2 thin film grown by ALD

Since the temperature window for our ALD chemistry is very low for the film to be crystallized, the films grown in this temperature range (100 ~ 120 °C) are characterized to be amorphous by TEM and XRD analysis (see Figs. 5b and Fig. 6). If the ALD MoS_2 films were completely amorphous, no clear peaks should be visible in Raman spectra.[38] However the Raman spectra in Fig. 3b reveal that the amorphous MoS_2 film grown on SiO_2/Si has a locally-ordered S-Mo-S unit with an atomic arrangement of 2H-MoS_2. In the 2H structure of molybdenite (naturally occurring MoS_2), an atomic plane of Mo is sandwiched between two atomic planes of S in a trigonal prismatic arrangement. For the bulk MoS_2, the characteristic E^1_{2g} (in-plane) and A_{1g} (out-of-plane) Raman modes appear at 383 and 408 cm^{-1}, respectively.[39,40]

The ALD MoS_2 films grown with a higher number of ALD cycles than 60 cycles clearly show the characteristic E^1_{2g} mode at 381 cm^{-1} and the A_{1g} mode at 406 cm^{-1}. However the film grown for 40 cycles does not show any MoS_2 peak as compared with the Raman spectrum of the SiO_2/Si substrate (the Si peak at 304 cm^{-1} was marked with an asterisk in Fig. 3b). The E^1_{2g} and A_{1g} peaks also show a significant red-shift of 2 cm^{-1} and broadening of the characteristic modes comparing to the bulk MoS_2. While the bulk or few-layered MoS_2 generally show a line width (full width at half maximum, FWHM) ranged in 2 ~ 6 cm^{-1} for both peaks,[40] the FWHM (12~14 cm^{-1}) of ALD MoS_2 films is much broader. It is possibly due to the locally-ordered microstructure. Recently, it is reported that the E^1_{2g} and A_{1g} peaks can be shifted down and broadened for nanoparticles.[11,41,42]

Nanoscale Accepted Manuscript

Generally, the number of S-Mo-S layers in MoS_2 can be determined from the wavenumber difference (Δ) between E^1_{2g} and A_{1g} peaks, because the frequency of the former decreases and that of the latter increases with the number of layers.[40] For MoS_2 films with a higher number of layers than 5 ~ 6 layers, the Δ values are around 25 cm^{-1}. Even though the as-grown film by ALD does not show the layered crystalline structure in TEM and XRD analyses, since the thicknesses of the as-grown MoS_2 films with Raman peaks are thicker than 6 nm, the Δ values of them are also around 25 cm^{-1} as expected.

One more concern for the Raman spectra is the broad peak at 227 cm^{-1} marked with D in Fig. 3b. Although there is no Raman active mode for crystalline MoS_2 in the wavenumber region,[39] the D peak appears only when the E^1_{2g} and A_{1g} peaks are observed. Raman inactive modes due to the Raman selection rule can be activated when the crystal symmetry is broken by defects.[41,42] We believe that the D peak may be attributed to the disorder in the microstructure of MoS_2 film. This behavior seems to be analogous to the disorder-induced mode found in graphitic carbon materials.[43,44] Similar results were also reported in deposited MoS_2 films by pulsed laser deposition.[45] They found that the intensity of the disorder peak (D) was relatively attenuated compared to the intensity of the A_{1g} peak by annealing the samples because the crystallinity was improved.

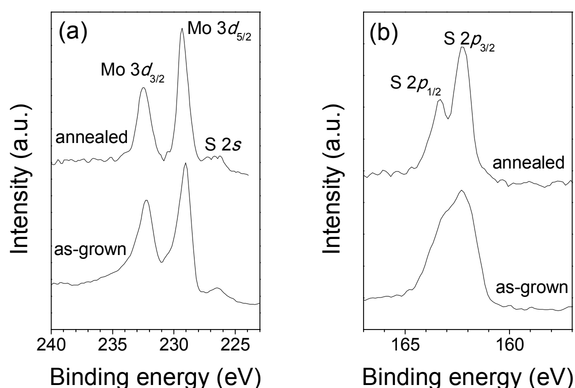

Fig. 4. XPS spectra of MoS_2 films as-grown by ALD or annealed at 900 °C for 5 min: Mo 3*d* (a) and S 2*p* (b) peaks. The binding energies were calibrated by using the C 1*s* peak (284.8 eV) of the adventitious carbon as an internal standard.

The as-grown MoS_2 film was also characterized by X-ray photoelectron spectroscopy (XPS) as shown in Fig. 4. The spectra was obtained on the surface sputtered by 2 keV Ar^+ for 3s in order to remove the adventitious carbon. The characteristic binding energies of Mo $3d_{3/2}$ and $3d_{5/2}$, which are attributed to Mo^{4+}, were observed at 232.3 and 229.1 eV, respectively.[38,46] For the binding energies of S $2p_{1/2}$ and $2p_{3/2}$ for divalent sulfide ion (S^{2-}), the $2p_{3/2}$ peak was observed at 162.3 eV, and the $2p_{1/2}$ peak was not clearly resolved but appeared as a shoulder of the $2p_{3/2}$ peak. These binding energy values are consistent with the previous reports for MoS_2.[38,46] However the stoichiometric ratio of S/Mo is estimated to be 1.21 for the as-grown film, possibly due to partial oxidation of the surface. Indeed, high oxygen content is detected on the surface with an O/S ratio of 0.85 while carbon content is negligible (~ 0.1 at%). Furthermore the oxygen concentration in the as-grown film rapidly decreases during XPS depth profiling (See Fig. S1 in ESI). This supports the partial oxidation of the surface due to vulnerable nature of the as-grown film in air.

In order to crystallize amorphous MoS_2, the as-grown film was annealed at 900 °C for 5 min under Ar atmosphere. The XPS spectra of the annealed film are also shown in Fig 4, the Mo $3d_{3/2}$ and $3d_{5/2}$ peaks are located at 232.5 and 229.3 eV, respectively, and the S 2*p* doublet is clearly resolved at 163.3 and 162.2 eV after the annealing. In addition, the stoichiometric ratio of S/Mo is 2.01 and both oxygen and carbon atoms are not detected on the annealed film.

After the annealing, the Raman modes become much stronger and narrower (FWHM ~9 cm^{-1}), comparing to the as-grown film (Fig. 5a). The D peak at 227 cm^{-1}, originated from the disorder of MoS_2, is also relatively attenuated comparing to that of the as-grown film. But the Δ value was not changed due to its 15 nm-thick thickness. For the same specimen, we investigated the crystal structure by XRD and high resolution TEM. The strong peak (2θ = 14.27) in Fig. 5b is attributed to (002) basal planes of which interplanar spacing (d_{002}) is calculated to be ~0.625 nm from the 2θ value. This indicates a little expansion (~1.7 %) of the layer spacing in comparison to that (0.615 nm) of molybdenite.[47] Cross-sectional high resolution TEM image (Fig. 6) also shows that the S-Mo-S layers are aligned with the (002) basal plane parallel to the substrate. The averaged d_{002} obtained from the TEM image is around 0.63 nm which is also consistent with the d_{002} value obtained by XRD. The crystallization of MoS_2 in the parallel direction of the substrate will be advantageous to prepare electronic devices based on MoS_2 such as transistors. However since the film is not fully crystallized in its thickness due to the short annealing time (5 min), the crystallization process of the as-grown film should be optimized for the device fabrication.

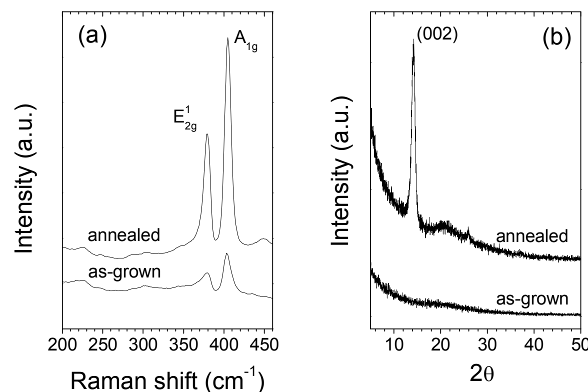

Fig. 5. Raman spectra (a) and XRD patterns (b) of MoS_2 films as-grown by ALD or annealed at 900 °C for 5 min.

Nanoscale Accepted Manuscript

 This journal is © The Royal Society of Chemistry 2012

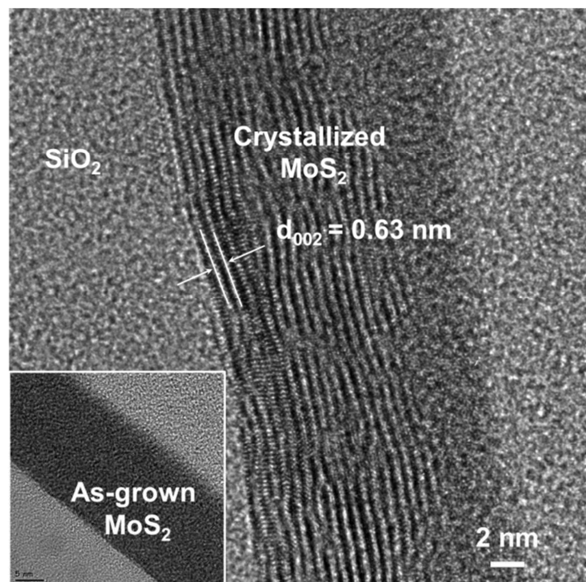

Fig. 6. Cross-sectional high resolution TEM image of MoS_2 film annealed at 900 °C for 5 min. The TEM image in the inset shows an amorphous nature of the as-grown film.

4 Conclusions

In summary, we propose a novel chemical route for MoS_2 ALD using $Mo(CO)_6$ and DMDS as Mo and S precursors, respectively. $Mo(CO)_6$ is chemically adsorbed to be $Mo(CO)_n$ ($n \leq 5$) in the first-half reaction, and the methylthiolate intermediate from the dissociative chemisorption of DMDS in the second-half reaction may undergo additional decomposition to produce sulfur adatoms, possibly owing to the catalytic effect of the chemisorbed $Mo(CO)_n$. Even though the as-grown film is amorphous due to the low growth temperature (100 °C), it clearly shows the characteristic Raman modes (E^1_{2g} and A_{1g}) of MoS_2. The as-grown amorphous MoS_2 may be utilized for catalysis applications such as electrochemical HER. In addition, the crystallized MoS_2 by annealing may be used for the electronic applications, since the annealing process results in crystallization of the (002) basal planes in a parallel direction to the SiO_2/Si substrate.

Acknowledgements

This work was supported by Konkuk University in 2012. The authors thank to H. K. Kang and M. K. Cho (Advanced Analysis Center, KIST) for XPS and TEM analyses, respectively.

Notes and References

[a] Department of Chemical Engineering, Konkuk University, 120 Neungdong-Ro, Gwangjin-Gu, Seoul 143-701, Korea

† These authors equally contributed to this work.

‡ Electronic Supplementary Information (ESI) available: XPS depth profiles for the as-grown and the annealed MoS_2 films. See DOI: 10.1039/b000000x/

1 Geim, A. K. *Science* **2009**, *324*, 1530.
2 Butler, S. Z. et al. *ACS Nano*, **2013**, *7*, 2898.
3 Chhowalla, M.; Shin, H. S.; Eda, G.; Li, L. J.; Loh, K. P.; Zhang, H. *Nat. Chem.* **2013**, *5*, 263.
4 Wang, Q. H.; Kalantar-Zadeh K.; Kis, A.; Coleman, J. N.; Strano, M. S. *Nat. Nanotech.* **2012**, *7*, 699.
5 Yang, J.; Shin, H. S. *J. Mater. Chem. A* **2014**, *2*, 5979.
6 Mak, K. F.; Lees, C.; Hone, J.; Shan, J.; Heinz, T. F. *Phys. Rev. Lett.* **2010**, *105*, 136805.
7 Novoselov, K. S.; Jiang, D.; Schedin, F.; Booth, T. J.; Khotkevich, V. V.; Morozov, S. V.; Geim, A. K. *Proc. Nat. Acad. Sci.* **2005**, *102*, 10451.
8 Radisavljevic, B.; Radenovic, A.; Brivio, J.; Giacometti, V.; Kis, A. *Nat. Nanotech.* **2011**, *6*, 147.
9 Das, S.; Chen, H. Y.; Penumatcha, A. V.; Appenzeller, J. *Nano Lett.* **2013**, *13*, 100.
10 Jaramillo, T. F.; Jorgensen, K. P.; Bonde, J.; Nielsen J. H.; Horch, S.; Chorkendorff, I. *Science* **2007**, *317*, 100.
11 Li, Y.; Wang, H.; Xie, W. L.; Liang, Y.; Hong G.; Dai, H. *J. Am. Chem. Soc.* **2011**, *133*, 7296.
12 Schwierz, F. *Proc. IEEE* **2013**, *101*, 1567.
13 Lee, Y. H.; Zhang, X. Q.; Zhang, W.; Chang, M. T.; Lin, C. T.; Chang, K. D.; Yu, Y. C.; Wang, J. T. W.; Chang, C. S.; Li, L. J.; Lin, T. W. *Adv. Mater.* **2012**, *24*, 2320.
14 Zhan, Y.; Liu, Z.; Najmaei, S.; Ajayan, P. M.; Lou, J. *Small* **2012**, *8*, 966.
15 Wang, X.; Feng, H.; Wu, Y.; Jiao, L. *J. Am. Chem. Soc.* **2013**, *135*, 5304.
16 Yu, Y.; Li, C.; Liu, Y.; Su, L.; Zhang, Y.; Cao, L. *Sci. Rep.* **2013**, *3*, 1866.
17 Meyer, B. *Chem. Rev.* **1976**, *76*, 367.
18 George, S. M. *Chem. Rev.* **2010**, *110*, 111.
19 Diskus, M.; Nilsen, O.; Fjellvag, H. *J. Mater. Chem.* **2011**, *21*, 705.
20 Seghete, D.; Rayner, Jr., G. B.; Cavanagh, A. S.; Anderson, V. R.; George, S. M. *Chem. Mater.* **2011**, *23*, 1668.
21 Wang, H.; Lu, Z.; Xu, S.; Kong, D.; Cha, J. J.; Zheng, G.; Hsu, P. C.; Yan, K.; Bradshaw, D.; Prinz, F. B.; Cui, Y. *Proc. Nat. Acad. Sci.* **2013**, *110*, 19701.
22 Tan, L. K.; Liu, B.; Teng, J. H.; Guo, S.; Low, H. Y.; Loh, K. P. *Nanoscale*, DOI: 10.1039/C4NR02451F.
23 Yim, C.; O'Brien, M.; McEvoy, N.; Winters, S.; Mirza, I.; Lunney, J. G.; Duesberg, G. S. *Appl. Phys. Lett.* **2014**, *104*, 103114.
24 Ohta, T.; Cicoira, F.; Doppelt, P.; Beitone, L.; Hoffmann, P. *Chem. Vap. Dep.* **2001**, *7*, 33.
25 Chellappa, R.; Chandra, D. *J. Chem. Thermodynamics* **2005**, *37*, 377.
26 Cross, J. S.; Schrader, G. L. *Thin Solid Films* **1995**, *259*, 5.
27 Gesheva, K. A.; Ivanova, T. *Chem. Vap. Dep.* **2006**, *12*, 231.
28 Reddy, K.; Brown, T. L. *J. Am. Chem. Soc.* **1995**, *117*, 2845.
29 Huang, H. H.; Sreekanth, C. S.; Seet, C. S.; Jiang, X.; Xu, G. Q. *Surf. Sci.* **1996**, *365*, 769.
30 Jiang, Z.; Xu, L.; Huang, X. *J. Mol. Catal. A* **2009**, *304*, 16.
31 Kruger, P.; Petukhov, M.; Domenichini, B.; Berko, A.; Bourgeois, S. *J. Phys. Chem. C* **2012**, *116*, 10617.
32 Nuzzo, R. G.; Zegarski, B. R.; Dubois, L. H. *J. Am. Chem. Soc.* **1987**, *109*, 733.

Nanoscale Accepted Manuscript

33 Wiegand, B. C.; Friend, C. M. *Chem. Rev.* **1992**, *92*, 491.
34 Halevi, B.; Vohs, J. M. *Surf. Sci.* **2008**, *602*, 198.
35 Roper, M. G.; Jones, R. G. *Phsy. Chem. Chem. Phys.* **2008**, *10*, 1336.
36 Cometto, F. P.; Macagno, V. A.; Parcedes-Olivera, P.; Patrito, E. M.; Ascolani, H.; Zampieri, G. *J. Phys. Chem. C 2010*, **114**, 10183.
37 VonNiederhausern, D. M.; Wilson, G. M.; Giles, N. F. *J. Chem. Eng. Data* **2006**, *51*, 1990.
38 McDevitt, N. T.; Bultman, J. E.; Zabinski, J. S. *Appl. Spectro.* **1998**, *52*, 1160.
39 Verble, J. L.; Wieting, T. J. *Phys. Rev. Lett.* **1970**, *25*, 362.
40 Lee, C.; Yan, H.; Brus, L. E.; Heinz, T. F.; Hone, J.; Ryu, S. *ACS Nano* **2010**, *4*, 2695.
41 Frey, G. L.; Tenne, R.; Matthews, M. J.; Dresselhaus, M. S.; G. Dresselhaus, *Phys. Rev. B* **1999**, *60*, 2883.
42 Gaur, A. P. S.; Sahoo, S.; Ahmadi, M.; Guinel, M. J. F.; Gupta, S. K.; Pandey, R.; Dey, S. K.; Katiyar, R. S. *J. Phys. Chem. C* **2013**, *117*, 26262.
43 Min, Y. S.; Bae, E. J.; Oh, B. S.; Kang, D.; Park, W. *J. Am. Chem. Soc.* **2005**, *127*, 12498.
44 Bae, E. J.; Min, Y. S.; Ko, J. H.; Kang, D.; Park, W. *Chem. Mater.* **2005**, *17*, 5141.
45 McDevitt, N. T.; Zabinski, J. S.; Donley, M. S., Bultman, J. E. *Appl. Spectro.* **1994**, *48*, 733.
46 Merki, D.; Fierro, S.; Vrubel, H.; Hu, X. *Chem. Sci.* **2011**, *2*, 1262.
47 Schonfeld, B.; Huang, J. J.; Moss, S. C. *Acta Crystal. B,* **1983**, *39*, 404.

Nanoscale Accepted Manuscript

 This journal is © The Royal Society of Chemistry 2012